

Supplementary Methods and Results
Empowering the crowd: Feasible strategies
to minimize the spread of COVID-19
in informal settlements

Alberto Pascual-García^{(1,*),} Jordan Klein⁽²⁾, Jennifer Villers^(3,^),
Eduard Campillo-Funollet^(4,^), Chamsy Sarkis⁽⁵⁾

March 2, 2021

(1) Institute of Integrative Biology. ETH-Zürich. Zürich, Switzerland.

(2) Office of Population Research. Princeton University. Princeton, NJ, USA.

(3) Princeton Environmental Institute. Princeton University. Princeton, NJ, USA.

(4) Genome Damage and Stability Centre. University of Sussex. Brighton, United Kingdom.

(5) Pax Syriana Foundation. Valetta, Malta.

(^) Equal contribution.

(*) correspondence: alberto.pascual@env.ethz.ch

1 Parameterization of the model

1.1 Derivation of fixed parameters (Table 1 in Main Text)

To estimate the latent period ($1/\delta_E$), we calculated the difference between randomly generated incubation ($1/\delta_E + 1/\delta_P$) and presymptomatic ($1/\delta_P$) periods. We estimated the presymptomatic period using results reported by He et al. [1] and found they best fit a Gompertz distribution with a mean of 2.3 days (95% CI: 0.8-3.0). Since a correction of these by Ashcroft et al. [2] suggests they significantly underestimate the presymptomatic period's upper bound, we estimated that the true presymptomatic period follows a Gaussian distribution around the mean (95% CI: 0.8-3.8). However, this presymptomatic period distribution implies a non-negligible probability of a negative latent period. To correct this discrepancy, we assumed a minimum latent period of .5 days [3]. Time from symptom onset to death in critical cases ($1/\alpha$) is estimated using time from symptom onset to ICU admission in Wang et al [4].

1.2 Population structure of demographic-classes derivation (Table 2 in Main Text)

In April, 2020, 40.7% of the population in informal IDP camps in Northern Syria was aged 0-12, 53.4% aged 13-50, and 5.9% aged 51+ [5]. To estimate the proportion of each age group with comorbidities, we calculated the weighted average age-specific comorbidity prevalence of the 4 most common comorbidities in the Syrian refugee populations in Jordan and Lebanon: hypertension, cardiovascular disease, diabetes, and chronic respiratory disease [6, 7]. We standardized these weighted averages to the age structure of IDPs in Northern Syria and estimated that 11.7% of people aged 13-50 have comorbidities, while 62.9% of people aged 51+ have comorbidities.

1.3 Derivation of transmissibility parameters

The probability of infection if there is a contact between a susceptible and an infected person depends on the stage of the disease, denoted $\tau\beta_P$, $\tau\beta_A$, $\tau\beta_I$ or $\tau\beta_H$ depending upon whether the infected individual is in the presymptomatic (P_i), symptomatic (I_i), asymptomatic (A_i), or hospitalized compartment (H_i), respectively. We estimated these parameters in two steps. In the following section, we estimate the β_X parameters ($X \in \{P, A, I, H\}$) which represent the relative transmissibility of each stage with respect to the maximum transmissibility τ . After this calculation, we present our estimate for the maximum transmissibility parameter τ .

Relative transmissibilities β (Table 1 in Main Text)

We start by considering the transmissibility of the presymptomatic stage for those individuals becoming symptomatic as a reference ($\beta_{P \rightarrow I} = 1$), since the probability of infection from contact with an individual at this epidemiological stage is highest [8]. Next, we set the contribution of each epidemiological stage to infectivity as proportional to β_X/γ_X , with $1/\gamma_X$ the duration of stage X. Following He et al, we estimate the proportion of infectivity that occurs at the presymptomatic stage ($X \in \{P\}$) as the area under the infectivity curve prior to symptom onset, AUC_P , and the proportion of infectivity that occurs at symptomatic stages ($X \in \{I, H\}$) as the area under the infectivity curve after symptom onset, $1 - AUC_P$ [8]:

$$\frac{AUC_P}{(1 - AUC_P)} \approx \frac{\frac{\beta_{P \rightarrow I}}{\delta_P}}{\frac{\beta_I}{\gamma_I} + \frac{\beta_H}{\gamma_H}} \quad (1)$$

We then considered the quantity ρ_{HI} , the ratio of the viral culture positive test rate in hospitalized patients 7-16 days since start of symptoms to the positive test rate in patients 0-6 days since start of symptoms from van Kampen et al.[9]. Similarly, the relative risk of asymptomatic transmission to symptomatic transmission according to Byambasuren et al. is expressed as ρ_{AI} [10]:

$$\beta_A = \beta_I \rho_{AI} \quad (2)$$

$$\beta_H = \beta_I \rho_{HI} \quad (3)$$

Considering these relationships we rewrite Eq. 1 to obtain the desired parameters:

$$\beta_I = \frac{\beta_{P \rightarrow I} \gamma_I \gamma_H (1 - AUC_P)}{AUC_P \delta_P (\gamma_H + \rho_{HI} \gamma_I)} \quad (4)$$

$$\beta_A = \frac{\rho_{AI}\beta_{P \rightarrow I}\gamma_I\gamma_H(1 - AUC_P)}{AUC_P\delta_P(\gamma_H + \rho_{HI}\gamma_I)} \quad (5)$$

$$\beta_H = \frac{\rho_{HI}\beta_{P \rightarrow I}\gamma_I\gamma_H(1 - AUC_P)}{AUC_P\delta_P(\gamma_H + \rho_{HI}\gamma_I)}. \quad (6)$$

The values of AUC_P , ρ_{AI} and ρ_{HI} are presented in Table 1, and the values of β_X in Main Text. Since the derivation was made relative to presymptomatic individuals that will become presymptomatic, we should also estimate the transmissibility of all presymptomatic individuals (β_P), i.e. also including those that will be asymptomatic. Since the proportion of presymptomatic that will become symptomatic is known (encoded in f in Eqs. 21–29 in Main Text) we considered that the relative transmissibility between presymptomatic individuals becoming symptomatic, and those becoming asymptomatic, is the same than between symptomatic and asymptomatic individuals (ρ_{AI}). Following these considerations, the total transmissibility is computed as:

$$\beta_P = f\beta_{P \rightarrow I} + (1 - f)\rho_{AI}\beta_{P \rightarrow I}.$$

Parameter	Description	Value	Distribution	Reference
AUC_P	Presymptomatic area under infectivity curve	0.44 (95% CI: .30-.57)	Gaussian	[8]
ρ_{AI}	Ratio of asymptomatic to symptomatic infectiousness	0.58 (95% CI: .34-.99)	Lognormal	[10]
ρ_{HI}	Ratio of hospitalized to symptomatic infectiousness	0.48	-	[9]

Table 1: **Relative transmissibility parameters.**

Maximum transmissibility parameter τ

In the following, to simplify the notation we define $\kappa_i = (l_i\gamma_I + h_i\eta + g_i\alpha)$. To estimate the probability of infection if there is a contact between a susceptible and an infected individual (parameter τ) we proceed as follows [11, 12, 13]. We start by considering the subsystem containing the infected population:

$$\dot{E}_i = \lambda_i S_i - \delta_E E_i \quad (7)$$

$$\dot{P}_i = \delta_E E_i - \delta_P P_i \quad (8)$$

$$\dot{A}_i = (1 - f)\delta_P P_i - \gamma_A A_i \quad (9)$$

$$\dot{I}_i = f\delta_P P_i - \kappa_i I_i \quad (10)$$

$$\dot{H}_i = h_i\eta I_i - \gamma_H H_i. \quad (11)$$

For the sake of simplifying the notation, let us consider the following ordering of the variables in the vector $x = (E_1, \dots, E_M, P_1, \dots, P_M, A_1, \dots, A_M, I_1, \dots, I_M, H_1, \dots, H_M)$, with M the number of population classes. We are interested in the parameterization of the null model, which will serve as a baseline to estimate the parameter τ , which is initially unknown, but does not change when interventions are introduced. Considering the contacts matrix for the null model (Eq. ?? in Main Text), the rate of exposure becomes

$$\lambda_i = \frac{\tau}{N} \sum_{j=1}^M c_j (\beta_P P_j + \beta_A A_j + \beta_I I_j + \beta_H H_j).$$

In the following, we use bold symbols for vectors and matrices, and the symbols \odot and \oslash for the element-wise multiplication and division, respectively. Following this notation, the linearized system can be written in the form $\dot{\mathbf{x}} = (\mathbf{T} + \boldsymbol{\Sigma})\mathbf{x}$, where:

$$T = \tau \begin{bmatrix} 0 & \Theta_P & \Theta_A & \Theta_I & \Theta_H \\ 0 & 0 & 0 & 0 & 0 \\ 0 & 0 & 0 & 0 & 0 \\ 0 & 0 & 0 & 0 & 0 \\ 0 & 0 & 0 & 0 & 0 \end{bmatrix} \quad (12)$$

is the transmission matrix, with $\Theta_X = \beta_X \text{diag}(\mathbf{p} \odot \mathbf{c}) \mathbf{U}$, $\mathbf{p} = \mathbf{N}/N$, \mathbf{U} is the all-ones matrix of size M , and β_X the infectiousness of compartment X relative to the presymptomatic compartment (see Main Text for details). The transition matrix is

$$\Sigma = \begin{bmatrix} -\delta_E \mathbf{I} & \mathbf{0} & \mathbf{0} & \mathbf{0} & \mathbf{0} \\ \delta_E \mathbf{I} & -\delta_P \mathbf{I} & \mathbf{0} & \mathbf{0} & \mathbf{0} \\ \mathbf{0} & (1-f)\delta_P \mathbf{I} & -\gamma_A \mathbf{I} & \mathbf{0} & \mathbf{0} \\ \mathbf{0} & f\delta_P \mathbf{I} & \mathbf{0} & -\text{diag}(\boldsymbol{\kappa}) \mathbf{I} & \mathbf{0} \\ \mathbf{0} & \mathbf{0} & \mathbf{0} & \eta \text{diag}(\mathbf{h}) \mathbf{I} & -\gamma_H \mathbf{I} \end{bmatrix} \quad (13)$$

Where \mathbf{I} and $\mathbf{0}$ are the identity and null matrices of size M , and $\boldsymbol{\kappa} = \mathbf{l}\gamma_I + \mathbf{h}\eta + \mathbf{g}\alpha$. We next compute the inverse of the transition matrix

$$\Sigma^{-1} = \begin{bmatrix} -\frac{1}{\delta_F} \mathbf{I} & \mathbf{0} & \mathbf{0} & \mathbf{0} & \mathbf{0} \\ -\frac{1}{\delta_P} \mathbf{I} & -\frac{1}{\delta_P} \mathbf{I} & \mathbf{0} & \mathbf{0} & \mathbf{0} \\ -\frac{(1-f)}{\gamma_A} \mathbf{I} & -\frac{(1-f)}{\gamma_A} \mathbf{I} & -\frac{1}{\gamma_A} \mathbf{I} & \mathbf{0} & \mathbf{0} \\ -f \text{diag}(\boldsymbol{\kappa}^{-1}) \mathbf{I} & -f \text{diag}(\boldsymbol{\kappa}^{-1}) \mathbf{I} & \mathbf{0} & -\text{diag}(\boldsymbol{\kappa}^{-1}) \mathbf{I} & \mathbf{0} \\ -\frac{f\eta}{\gamma_H} \text{diag}(\mathbf{h} \oslash \boldsymbol{\kappa}) \mathbf{I} & -\frac{f\eta}{\gamma_H} \text{diag}(\mathbf{h} \oslash \boldsymbol{\kappa}) \mathbf{I} & \mathbf{0} & -\frac{\eta}{\gamma_H} \text{diag}(\mathbf{h} \oslash \boldsymbol{\kappa}) \mathbf{I} & -\frac{1}{\gamma_H} \mathbf{I} \end{bmatrix} \quad (14)$$

The NGM with large domain can now be found by $\mathbf{K}_L = -T\Sigma^{-1}$. However, since we know that each individual who gets infected becomes exposed (E compartment), we focus on the NGM with small domain, \mathbf{K}_S , which only consists of the E compartment [14]. We do this by removing the rows that correspond to the other compartments from T and the columns from Σ^{-1} . We then find:

$$\mathbf{K}_S = \tau \left[\frac{1}{\delta_P} \Theta_P + \frac{(1-f)}{\gamma_A} \Theta_A + f \text{diag}(\mathbf{h}^{-1}) \Theta_I + \frac{f\eta}{\gamma_H} \text{diag}(\mathbf{h} \oslash \boldsymbol{\kappa}) \Theta_H \right].$$

The reproduction number is related to the dominant eigenvalue of \mathbf{K}_S , i.e. $R_0 = |\lambda_1|$, and τ is estimated from the dominant eigenvalue of $\tilde{K}_S = K_S/\tau$. Considering the null model parameters $(\tilde{\lambda}_1^0)$, we have the expression:

$$\tau = \frac{R_0}{|\tilde{\lambda}_1^0|}. \quad (15)$$

1.4 Epidemiological severity proportions (Table 4 in Main Text)

In the Main Text, we presented the proportions in which clinical symptomatic individuals resolve into critical (q_i^D), severe (q_i^H) and recovered (q_i^R) cases. We assigned the fractions of symptomatic cases in children aged <13 that would become severe and critical from the fractions of symptomatic cases in children aged <11 that were severe and critical in China [15]. We assigned the class-specific fractions of symptomatic cases in adults that would become severe and critical based on age and comorbidity-specific fractions of symptomatic cases with known outcomes that required hospitalization, without and with ICU admission, respectively in the United States [16]. To account for poorer health among Syrian adults compared to their similarly aged peers in developed countries, estimates for US adults aged 19-64 were used for Syrian adults aged 13-50, while estimates for US adults aged 65+ were used for Syrian adults aged 51+.

Since the rates at which these individuals progress are different (η for H , α for D and γ_I for R) we introduced three parameters, h_i , g_i and l_i , to distribute individuals according to the desired proportions following the equations:

$$q_i^H = h_i \eta \kappa_i^{-1} \quad (16)$$

$$q_i^D = g_i \alpha \kappa_i^{-1} \quad (17)$$

$$q_i^R = 1 - q_i^H - q_i^D = l_i \gamma_I \kappa_i^{-1}, \quad (18)$$

where $\kappa_i = h_i \eta + g_i \alpha + l_i \gamma_I$. The system has three unknowns and three equations but one equation linearly depends on the other two, hence we introduce the constraint $l_i = 1 - h_i - g_i$ to solve the system as:

$$h_i = \frac{\alpha q_i^H}{\eta q_i^D} g_i, \quad (19)$$

$$g_i = \gamma_I \left(\frac{\alpha}{q_i^D} + \frac{\gamma_I \alpha q_i^H}{\eta q_i^D} + \gamma_I - \frac{\alpha q_i^H}{q_i^D} - \alpha \right)^{-1}. \quad (20)$$

2 Parameterization of the interventions (Table 5 in Main Text)

2.1 Safety zone

We considered the existence of a safety zone to protect a certain fraction, f_S , of the population, mostly those more vulnerable. In practice, this involves dividing the camp in two areas, a “green” zone (denoted g) for the protected population and an “orange” zone (o) for the exposed population, and dividing each demographic-class into two behaviour-classes for each respective zone. These two populations interact via a buffer zone, under controlled conditions where we assumed transmissivity is reduced by 80%, encoded in the parameter $\xi_{ij} = 0.2$. Each individual in the green zone can interact with a limited number (c_{visit}) of family members (hereafter “visitors”) from the orange zone per day. In some interventions we considered that individuals visiting the buffer zone will have a health check (e.g. temperature measurement), aimed at excluding symptomatic individuals. When the health check is applied, the probability of transmission by individuals in the I or H compartments from one zone to susceptible individuals from a different zone is set to zero (see parameters ζ_I and ζ_H in Eq. 10 in Main Text). In the following, we derive the values of parameters ϵ_{ij} and ω_{ij} , modifying the rate at which individuals become exposed (see Eq. 10 in Main Text).

Although setting up a safety zone implies a reduction in the number of contacts between classes of the green zone and the orange zone, the mean number of contacts that each individual has per day, c_i , is conserved. Therefore we need to estimate how contacts will be redistributed from individuals from a different zone to individuals living in the same zone. We model this redistribution of contacts with the parameter ϵ_{ij} :

$$\begin{aligned} \epsilon_{ij} &= \vartheta c_{\text{visit}} / c_i \quad (i, j \text{ in different zones}) \\ \epsilon_{ij} &= 1 - \vartheta c_{\text{visit}} / c_i \quad (i, j \text{ in same zone}). \end{aligned}$$

We define ϑ as¹:

$$\vartheta = \begin{cases} 1 & \text{if } i \in g \\ f_{o,\text{visit}} & \text{if } i \in o \end{cases}$$

If we assume that visitors are always different, the quantity $f_{o,\text{visit}} = c_{\text{visit}} \frac{N_g}{N_o}$ is the fraction of the orange population that visits the buffer zone.

Next, we estimate how the probability of interaction between a member of class i and class j is modified with respect to the null model, depending on the zones from which class i and class j are drawn. Suppose classes i and j are separated from the rest of the population and confined within a restricted zone. The probability that

¹If c_{visit} is large enough ($c_{\text{visit}} \approx 15$ contacts per day), ϑ should saturate, because every member of the orange zone would eventually visit the buffer zone, following the expression:

$$\vartheta = \begin{cases} 1 & \text{if } i \in g \\ f_{o,\text{visit}} \left(1 - \Theta(f_{o,\text{visit}} - 1) \frac{f_{o,\text{visit}} - 1}{f_{o,\text{visit}}} \right) & \text{if } i \in o \end{cases}$$

with the Heaviside function $\Theta(f_{o,\text{visit}} - 1) = 1$ if $f_{o,\text{visit}} \geq 1$. We chose values well below this saturation threshold (a maximum of 10 contacts per week, i.e. 1.42 contacts per day).

an individual of class i randomly encounters an individual of class j is larger in the restricted zone than in the previous setting, in which both classes had access to the whole camp mixed with individuals belonging to other classes. This modification of relative probability of interaction is encoded in the parameter ω_{ij} (see Eq. 10 in Main Text). More specifically, the proportion N_i/N of individuals of class i in the null model becomes N_i/N_X with N_X the total number of individuals in zone $X = \{o, g\}$. This yields the following values for ω_{ij} :

$$\begin{aligned}\omega_{ij} &= \left(\frac{N_i}{N_X}\right)/\left(\frac{N_j}{N_X}\right) = \frac{N}{N_X} \quad (i, j \text{ in same zone } X) \\ \omega_{ij} &= \left(\frac{N_i}{N_Y}\right)/\left(\frac{N_j}{N_Y}\right) = \frac{N}{N_Y} \quad (i \in X \text{ and } j \in Y).\end{aligned}$$

Scenario	Age 1, orange	Age 1, green	Age 2 no comorbidities, orange	Age 2 no comorbidities, green	Age 2 comorbidities, orange	Age 2 comorbidities, green	Age 3 no comorbidities, green	Age 3 comorbidities, green
Only age 3 in green zone	.407	0	.471	0	.0626	0	.022	.0373
Age 3 + age 2 with comorbidities in green zone	.407	0	.471	0	0	.0626	.022	.0373
20% green zone capacity	.376	.0312	.424	.0469	0	.0626	.022	.0373
25% green zone capacity	.356	.0512	.394	.0769	0	.0626	.022	.0373
30% green zone capacity	.336	.0712	.364	.107	0	.0626	.022	.0373

Table 2: **Fraction of population in each zone by safety zone scenario and behaviour-class.** Behaviour-classes that are not considered in a given scenario have a proportion equal to zero.

Following this parameterization, we explore different scenarios, summarized in Table 2, for allocating members of each population class to the safety, or “green” zone, and the exposed, or “orange” zone. In one scenario, we only place individuals in age group 3 (>50) in the green zone, while in another we place all vulnerable individuals, age group 3 and age group 2 (13-50) with comorbidities, in the green zone. In 3 additional scenarios, after all vulnerable individuals are allocated to the green zone, we set the green zone’s capacity to a certain percentage of the camp’s population (20%, 25%, 30%), and allocate its remainder to non-vulnerable family members, who by necessity are either children <13 in age group 1 or healthy younger adults in age group 2. In accordance with camp managers’ expectations that many vulnerable individuals will have non-vulnerable spouses, while fewer vulnerable individuals will have young children, in these scenarios we allocate 40% of the remainder of the green zone to children and 60% of the remainder of the green zone to younger adults without comorbidities. We also consider a baseline scenario in which there is no green zone.

2.2 Self-isolation and evacuation

To implement self-isolation we start expanding our model (Eqs 21–29 in Main Text) to consider a new compartment for each demographic-class. We split the clinical symptomatic compartment to model the fact that symptomatic individuals require some time to recognize their symptoms and to self-isolate. The symptomatic compartment is

split in two compartments: symptomatic prior to identification, O_i , and symptomatic following identification, I_i . Following these considerations, the structure of the model is represented in Fig. 1, which follows the equations:

$$\dot{S}_i = -\lambda_i S_i \quad (21)$$

$$\dot{E}_i = \lambda_i S_i - \delta_E E_i \quad (22)$$

$$\dot{P}_i = \delta_E E_i - \delta_P P_i \quad (23)$$

$$\dot{A}_i = (1-f)\delta_P P_i - \gamma_A A_i \quad (24)$$

$$\dot{O}_i = f\delta_P P_i - (l_i \gamma_I + h_i \delta_O + g_i \alpha) O_i \quad (25)$$

$$\dot{I}_i = \delta_O O_i - (l_i \gamma_I + h_i \eta' + g_i \alpha) I_i \quad (26)$$

$$\dot{H}_i = h_i (\eta' I_i + \delta_O O_i) - \gamma_H H_i \quad (27)$$

$$\dot{R}_i = \gamma_A A_i + l_i \gamma_I (I_i + O_i) + (1-\sigma) \gamma_H H_i \quad (28)$$

$$\dot{D}_i = g_i \alpha (I_i + O_i) + \sigma \gamma_H H_i \quad (29)$$

where the duration of O_i follows a Gaussian distribution with means $1/\delta_O \in \{12, 24, 48\}$ hours. The duration for which an individual spends in the clinical symptomatic compartment, $1/\eta'$, is then calculated as the difference between the symptomatic period if there is no isolation, $1/\eta$, and the duration spent in the symptom onset compartment ($1/\delta_O$). The remaining parameters determining the rate of change of individuals at O_i , namely the rate of progression towards recovery or death (γ_i and α) or the relative transmissibility, β_I remain the same than those of the symptomatic compartment, I_i .

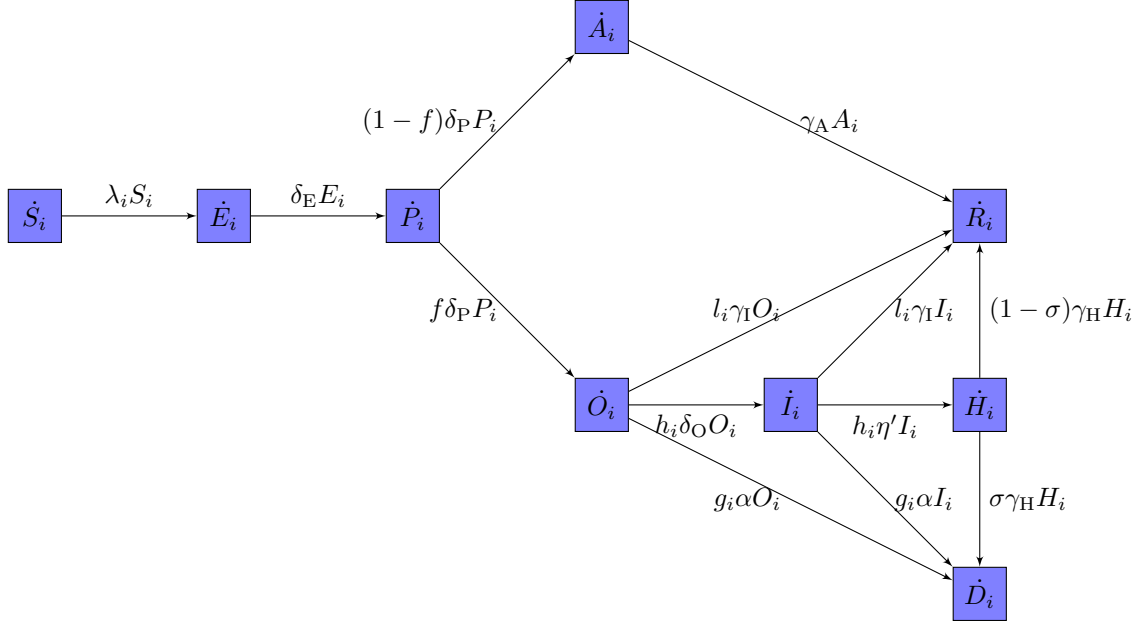


Figure 1: **Diagram of the model including the self-isolation intervention.** The model considers an additional symptom onset compartment (O).

The second modification required is a distinction between the isolated and non-isolated population within the clinical symptomatic compartment after identification of symptoms (I_i). The split in these two subpopulations is implemented computing, at each integration step in the simulation, the number of total infected individuals, $N_I = \sum_i I_i$. Next, we consider the isolation capacity of the camp (\tilde{N}), and we assumed that the number of isolated individuals for each class is proportional to the number of clinical symptomatic individuals in the class, i.e. $\tilde{I}_i = \tilde{N} I_i / N_I$. Note that, in doing this, we are not creating compartments, we are simply identifying the number of individuals that this class has under isolation. Once their numbers are determined, we just need to focus on the fact that the two subpopulations (isolated and not isolated) have a different number of contacts and

exposure to the other classes, which can be implemented in λ_i . A similar reasoning can be applied for the third and final consideration regarding the existence of carers, which are individuals from the younger adults class with no comorbidities. We do not create a new class, because all the epidemiological parameters of carers and those of younger adults with no comorbidities are identical and, hence, the only modification required concerns the rate of exposure. Therefore, we proceed by estimating the parameterization of λ_i following the intervention, in particular the values of ϵ_{ij} and ω_{ij} (see Eq 10 in Main Text).

Let us start considering the rate of exposure of the younger adults with no comorbidities, whose parameters are hereafter indicated with the index k . If this class has a number N_{care} of carers, and each isolated individual requires having c_{care} contacts per day with them and, if at a given stage of the disease each class j has \tilde{I}_j isolated individuals, the mean number of contacts that each carer has per day with individuals in isolation is $\tilde{c}_k = c_{\text{care}} \sum_j \tilde{I}_j / N_{\text{care}}$. We envisage these interactions occurring in what we call buffer zones, namely open spaces in which carers and isolated individuals maintain a distance and wear masks, reducing the transmissibility by 80% ($\xi = 0.2$). Given these assumptions, a general expression for the rate of exposure of the younger adults with no comorbidities, λ_k , is given by

$$\lambda_k^{\text{care}} = \tau \sum_j \underbrace{\xi \beta_I \tilde{c}_k \tilde{P}(k \rightarrow j)}_{\text{isolated}} + c_k \underbrace{\left(\frac{N_j - \tilde{I}_j}{N} \right) \left(\frac{\beta_P P + \beta_A A_j + \beta_I O_i + \beta_I \Theta(N_I - \tilde{N})(I_j - \tilde{I}_j) + \beta_H H_j}{N_j - \tilde{I}_j} \right)}_{\text{not isolated}}, \quad (30)$$

where $\tilde{P}(k \rightarrow j)$ is the probability that an individual of class k encounters an isolated individual of class j . For the not-isolated term, we maintain the well-mixed population assumption explained in the Main Text, with the incorporation of a Heaviside function, $\Theta(N_I - \tilde{N})$, which activates the interaction with the clinical symptomatic individuals when their number N_I exceeds the isolation capacity \tilde{N} , and we estimate the probability of interacting with non-isolated individuals to be proportional to their fraction $(I_j - \tilde{I}_j)/(N_j - \tilde{I}_j)$. For the isolated population, however, the well-mixed assumption is no longer valid, because carers will certainly interact with isolated individuals through their role as carers, hence $\tilde{P}(k \rightarrow j) = 1$. This yields the following expression for the subpopulation of carers

$$\lambda_k^{\text{care}} = \tau \sum_j \underbrace{\xi \beta_I \tilde{c}_k}_{\text{isolated}} + c_k \underbrace{\left(\frac{N_j - \tilde{I}_j}{N} \right) \left(\frac{\beta_P P + \beta_A A_j + \beta_I O_i + \beta_I \Theta(N_I - \tilde{N})(I_j - \tilde{I}_j) + \beta_H H_j}{N_j - \tilde{I}_j} \right)}_{\text{not isolated}},$$

Note that the mean number of contacts per day that carers have with the rest of the population, c_k , is not reduced. In doing so, we concentrate on the reduction in the transmissibility that the intervention has, and we do not incorporate further assumptions regarding changes in carers life-styles.

Those individuals belonging to the younger adults with no comorbidities not belonging to the group of carers will not interact with isolated individuals (i.e. $\tilde{P}(k \rightarrow j) = 0$), and hence their rate of exposure becomes:

$$\lambda_k^{\overline{\text{care}}} = c_k \underbrace{\left(\frac{N_j - \tilde{I}_j}{N} \right) \left(\frac{\beta_P P + \beta_A A_j + \beta_I O_i + \beta_I \Theta(N_I - \tilde{N})(I_j - \tilde{I}_j) + \beta_H H_j}{N_j - \tilde{I}_j} \right)}_{\text{not isolated}}. \quad (31)$$

The total rate of exposure of the younger adults with no comorbidities, then becomes:

$$\lambda_k = \frac{N_{\text{care}}}{N_k} \lambda_k^{\text{care}} + \left(\frac{N_k - N_{\text{care}}}{N_k} \right) \lambda_k^{\overline{\text{care}}},$$

which we can make explicit and simplify to yield

$$\lambda_k = \tau \sum_j \underbrace{\xi \beta_I c_{\text{care}} \frac{\tilde{I}_j}{N_k}}_{\text{isolated}} + c_k \underbrace{\left(\frac{\beta_P P + \beta_A A_j + \beta_I O_i + \beta_I \Theta(N_I - \tilde{N})(I_j - \tilde{I}_j) + \beta_H H_j}{N} \right)}_{\text{not isolated}}. \quad (32)$$

In our simulations, we consider that each isolated individual requires just one contact with carers, i.e. $c_{\text{care}} = 1$. Interestingly, the expression is independent of N_{care} , but the transmissibility of the isolated population inversely

depends on the size of the class hosting carers, suggesting that a small dedicated class would be optimal for the success of this intervention. We can express this equation following the parameterization presented in Eq. 10 in Main Text by choosing $\epsilon_{ij} = (c_{\text{care}}/c_i)(\tilde{I}_j/N_k)$ and $\omega_{ij} = N/N_k$ for the isolated population, while for the population not isolated it is not required any further parameterization ($\epsilon_{ij} = 1$ and $\omega_{ij} = 1$). The rate of exposure of the remaining classes ($i \neq k$) corresponds to the second term in the r.h.s of Eq. 32:

$$\lambda_i = \tau \sum_j c_i \underbrace{\frac{\beta_P P + \beta_A A_j + \beta_I \Theta(N_I - \tilde{N})(I_j - \tilde{I}_j) + \zeta_H \beta_H H_j}{N}}_{\text{not isolated}}.$$

3 Supplementary figures

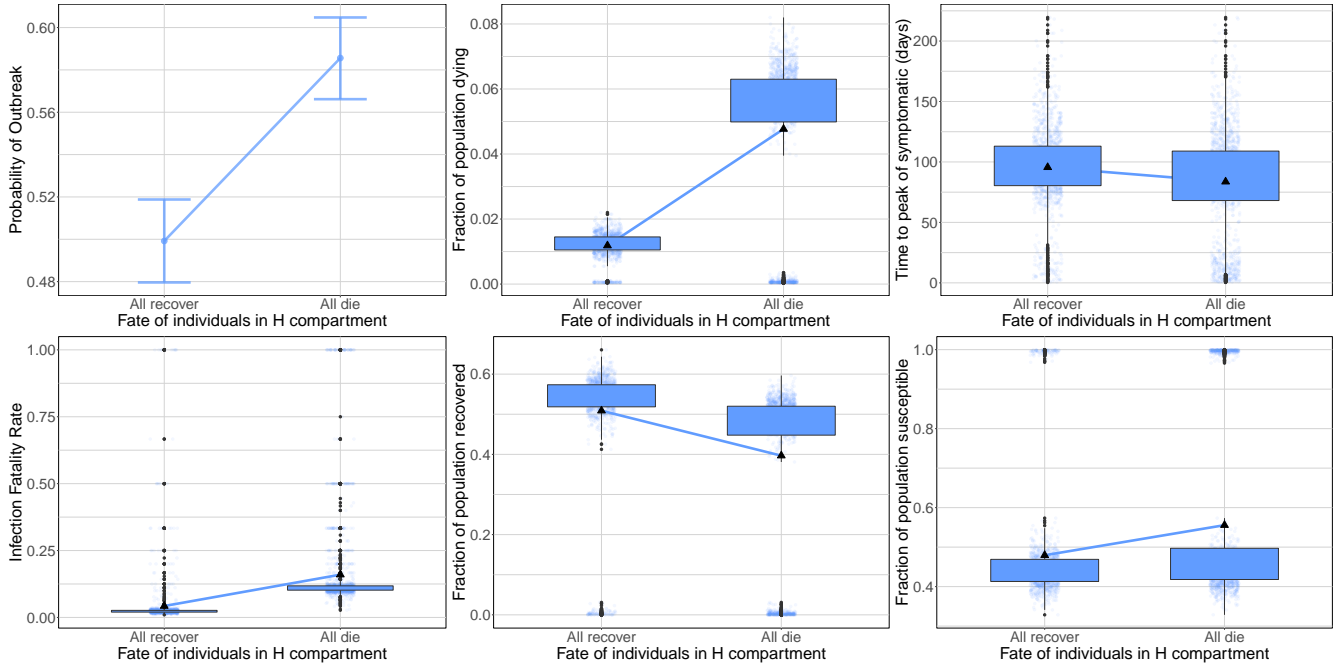


Figure 2: **Outcomes when all severe (hospitalized) cases recover ($\sigma = 0$) vs when all severe (hospitalized) cases die ($\sigma = 1$)**. Probability of an outbreak (top left), fraction of the population dying (top middle), time until peak symptomatic cases (top right), IFR (bottom left), and fraction of the population that recovers (bottom middle). Since we define outbreaks as simulations in which at least one person dies and probability of a case dying is higher when $\sigma = 1$, the probability of observing an outbreak is also necessarily higher when $\sigma = 1$.

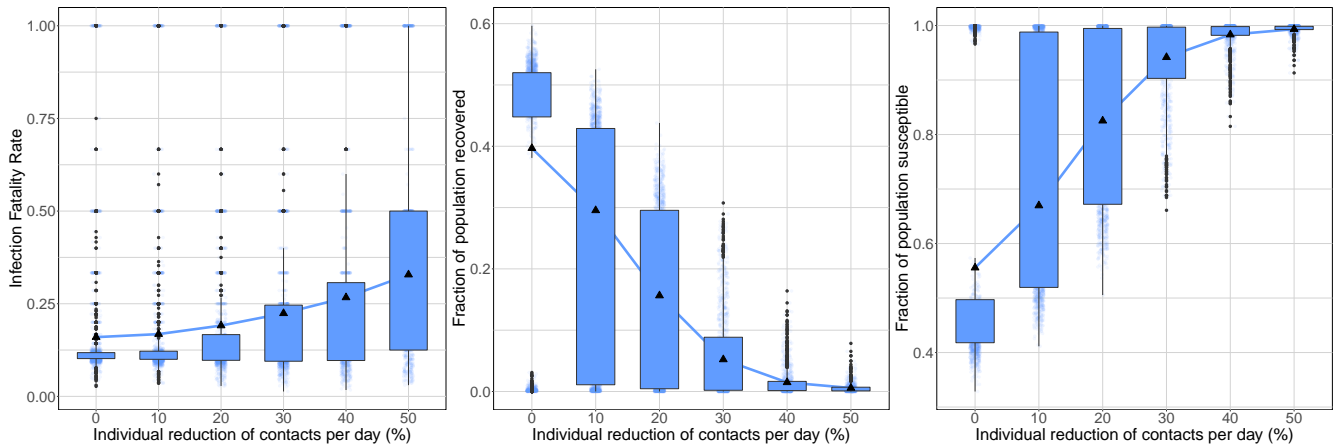


Figure 3: **Self-distancing.** IFR (left), and fraction of the population that recovers (right) as a function of the proportion of contacts reduced per individual per day.

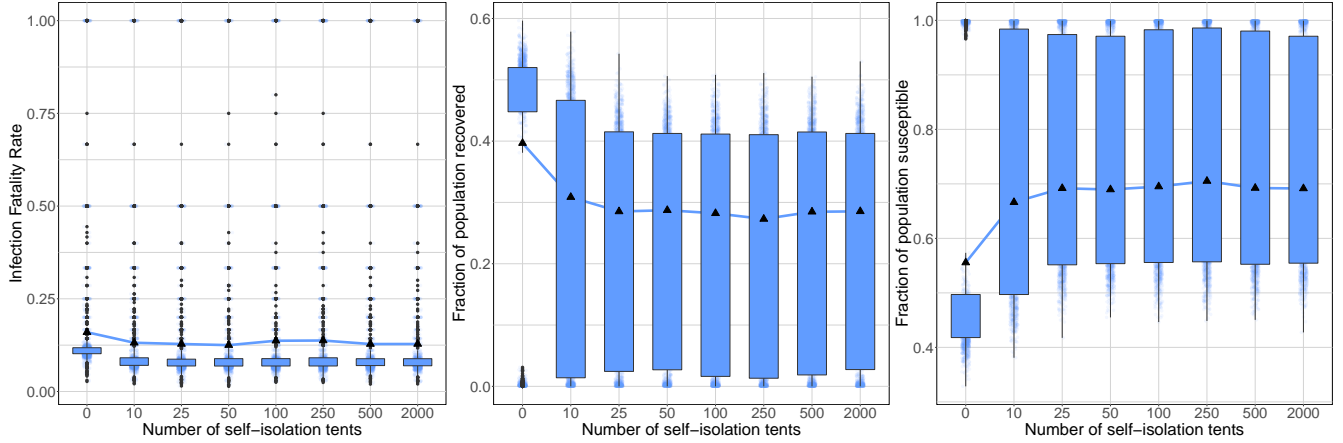


Figure 4: **Self-isolation.** IFR (left), and fraction of the population that recovers (right) as a function of the number of isolation tents available in the camp.

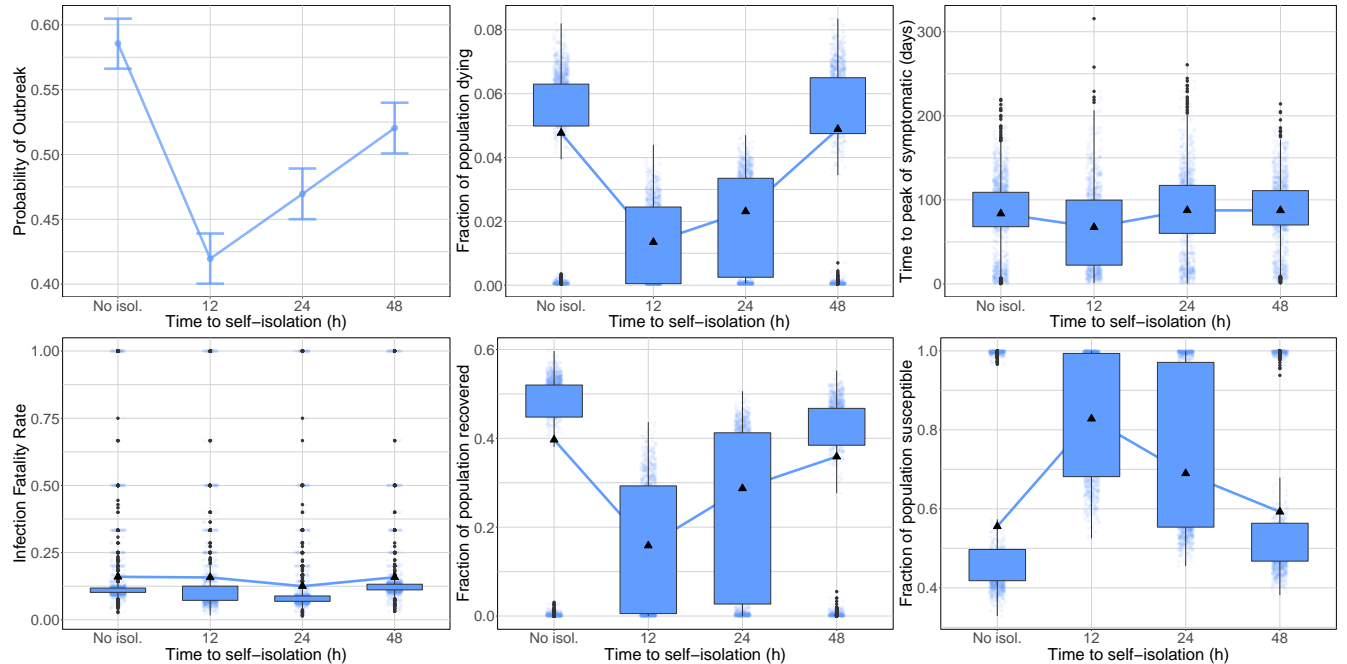


Figure 5: **Time to self-isolation.** Probability of an outbreak (top left), fraction of the population dying (top middle), time until peak symptomatic cases (top right), IFR (bottom left), and fraction of the population that recovers (bottom middle) as a function of the time that individuals require to recognize their symptoms and self-isolate. The isolation capacity

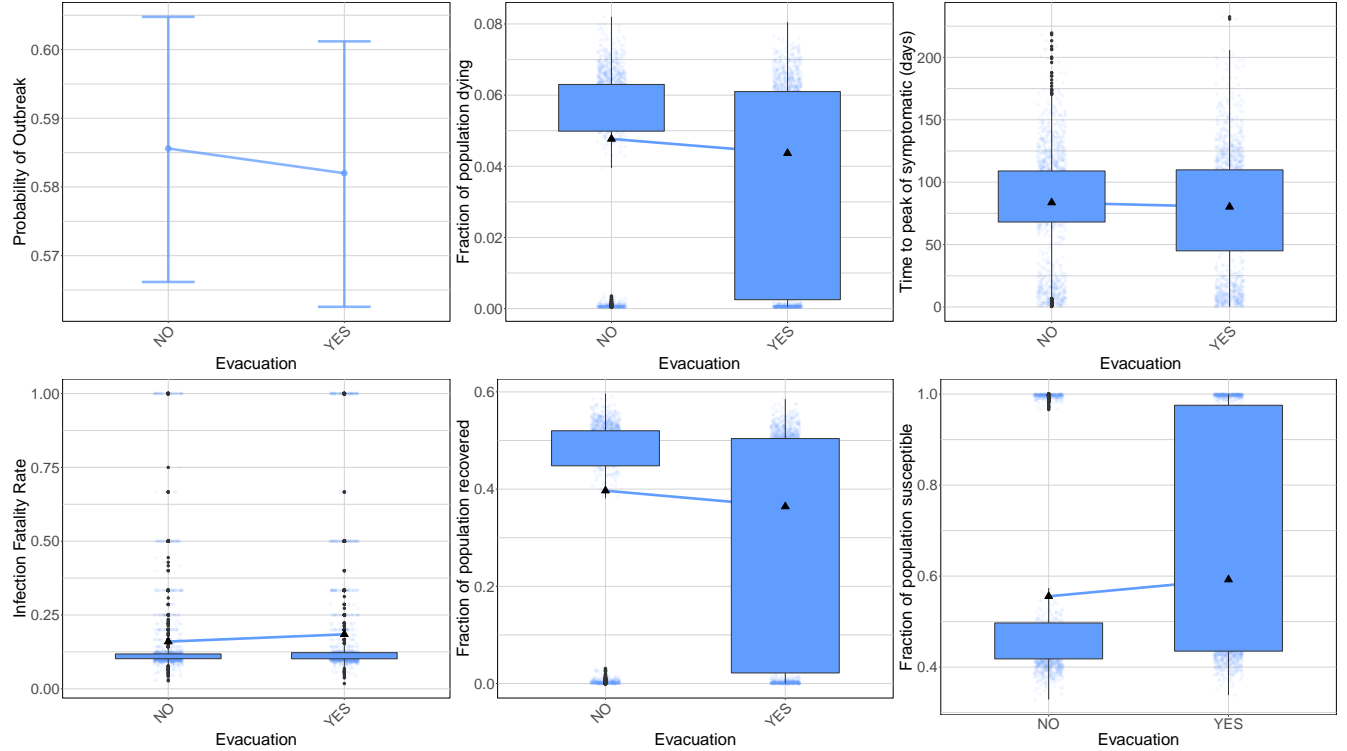


Figure 6: **Evacuation.** Probability of an outbreak (top left), fraction of the population dying (top middle), time until peak symptomatic cases (top right), IFR (bottom left), and fraction of the population that recovers (bottom middle), as a function of whether individuals requiring hospitalization are evacuated to isolation centers.

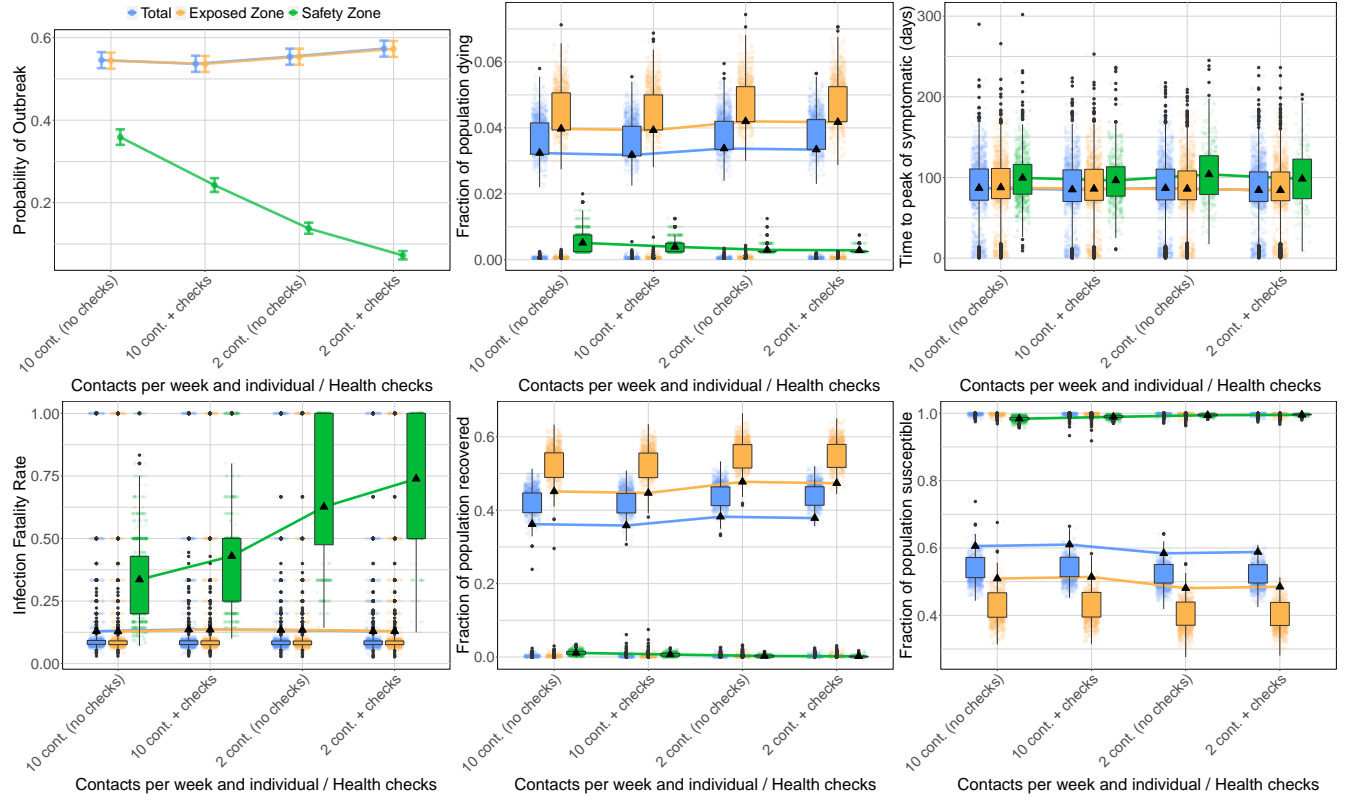


Figure 7: Health-checks in the buffer zone. Probability of an outbreak (top left), fraction of the population dying (top middle), time until peak symptomatic cases (top right), IFR (bottom left), and fraction of the population that recovers (bottom middle), as a function of whether health-checks are implemented in the buffer zone between the safety and exposed zones. Scenarios with 10 or 2 contacts in the buffer zone per person in the safety zone per week are plotted. All figures consider the scenario in which 20% of the camp's population is allocated to the safety zone.

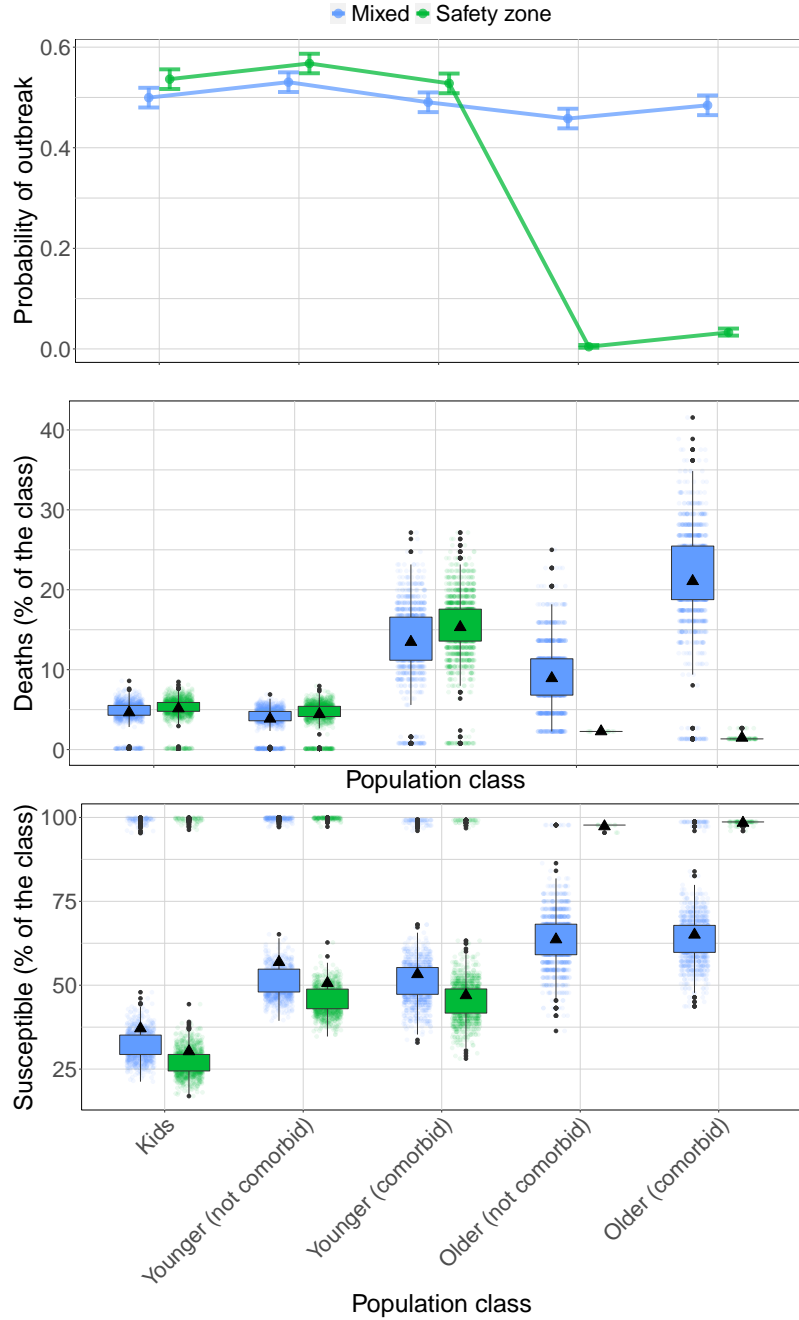


Figure 8: Effects of the safety zone on outcomes by population class. Probability of an outbreak (top), and proportion that dies in each population class (bottom) when no interventions are implemented (Mixed), compared to protection of older adults in the safety zone with 2 contacts in the buffer zone per week (Safety zone). The fraction of deaths in the safety zone for the older population is significantly lower (Kruskal-Wallis test, $p\text{-val} < 10^{-15}$).

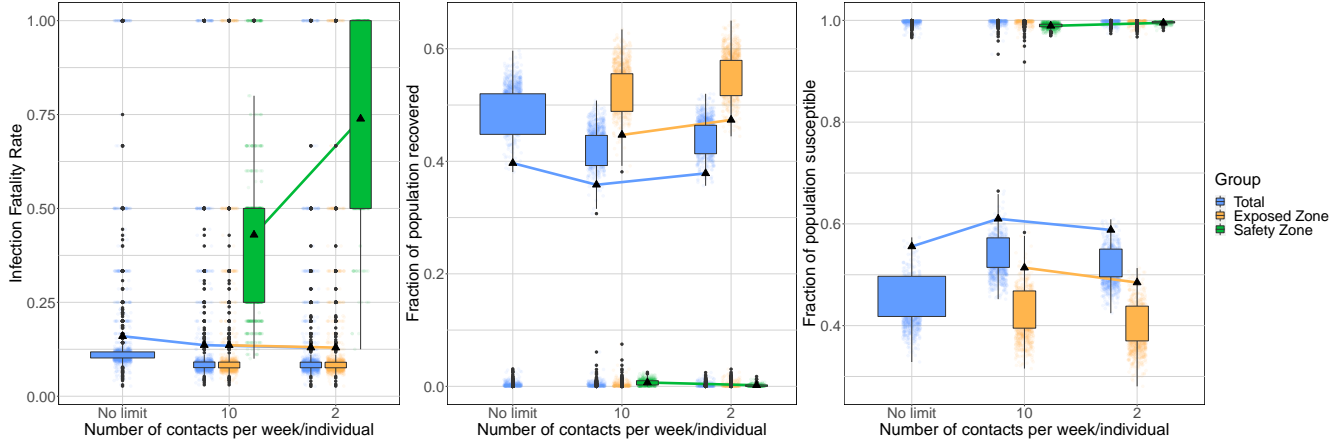


Figure 9: **Number of contacts in the buffer zone.** IFR (left), and fraction of the population that recovers (right) as a function of the number of contacts that each individual in the safety zone has in the buffer zone per week. All figures consider the scenario in which 20% of the camp's population is allocated to the safety zone.

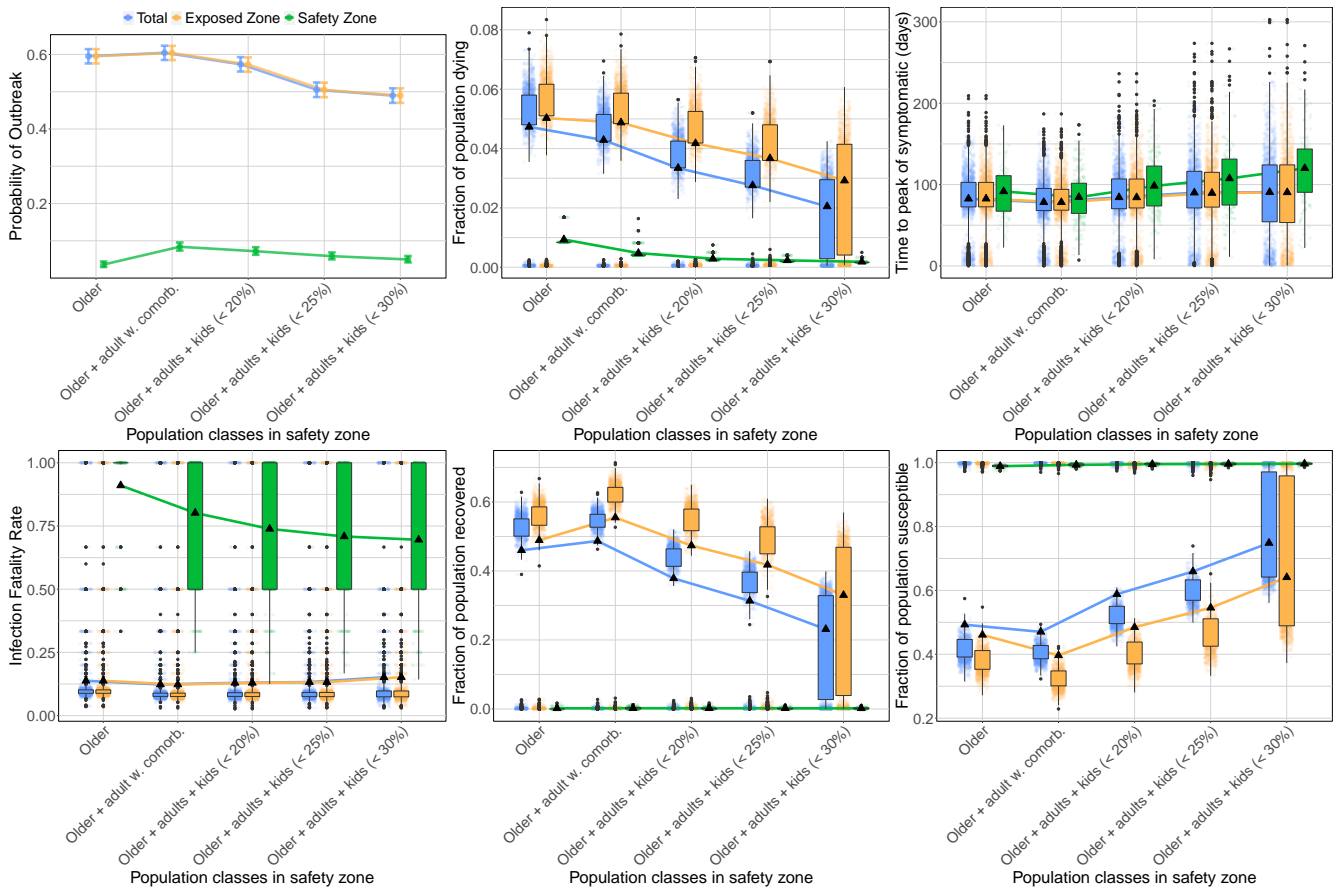


Figure 10: **Population moving to the safety zone.** Probability of an outbreak (top left), fraction of the population dying (top middle), time until peak symptomatic cases (top right), IFR (bottom left), and fraction of the population that recovers (bottom middle) as a function of the safety zone allocation scenario (see Table 2). All figures consider the scenario with 2 contacts in the buffer zone per person in the safety zone per week.

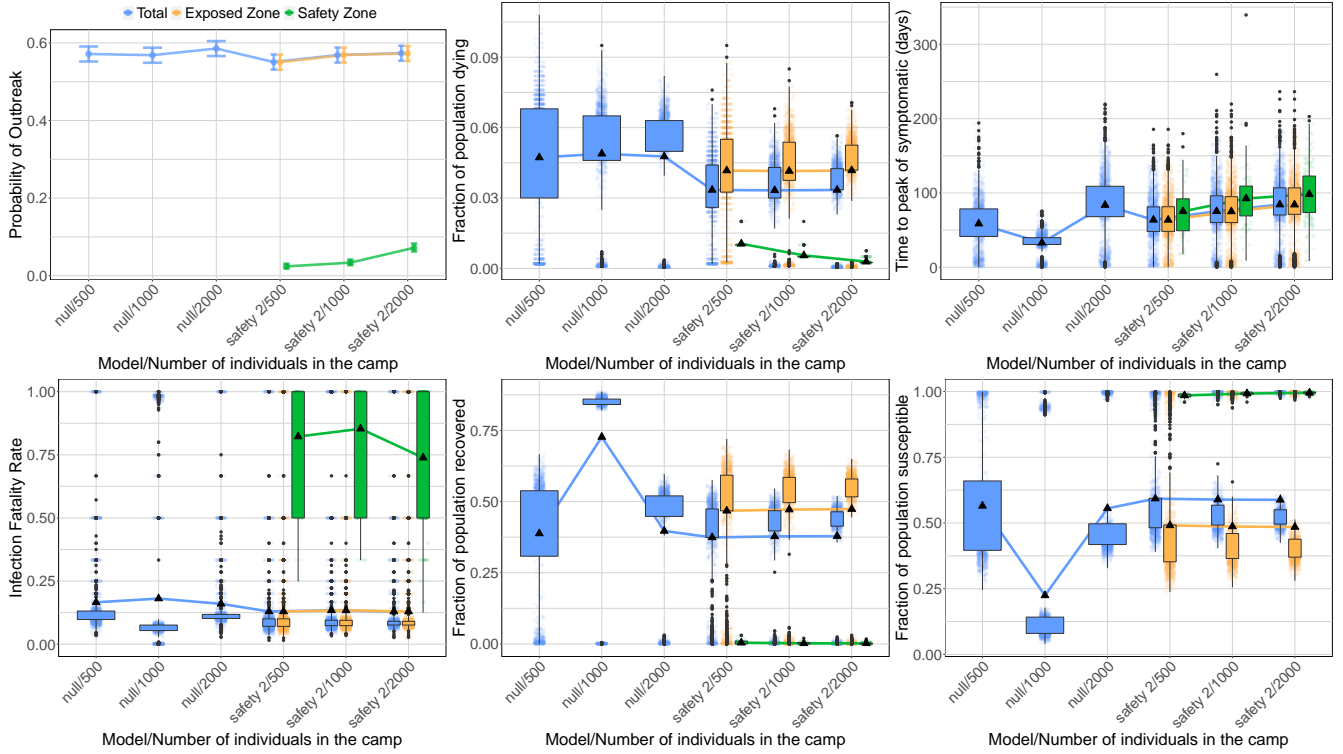


Figure 11: **Efficacy of the safety zone for different population sizes.** Probability of an outbreak (top left), fraction of the population dying (top middle), time until peak symptomatic cases (top right), IFR (bottom left), and fraction of the population that recovers (bottom middle) as a function of the total population size. The figures consider scenarios with no interventions (null), and with a safety zone comprising 20% of the camp's population with 2 contacts in the buffer zone per person in the safety zone per week (safety 2).

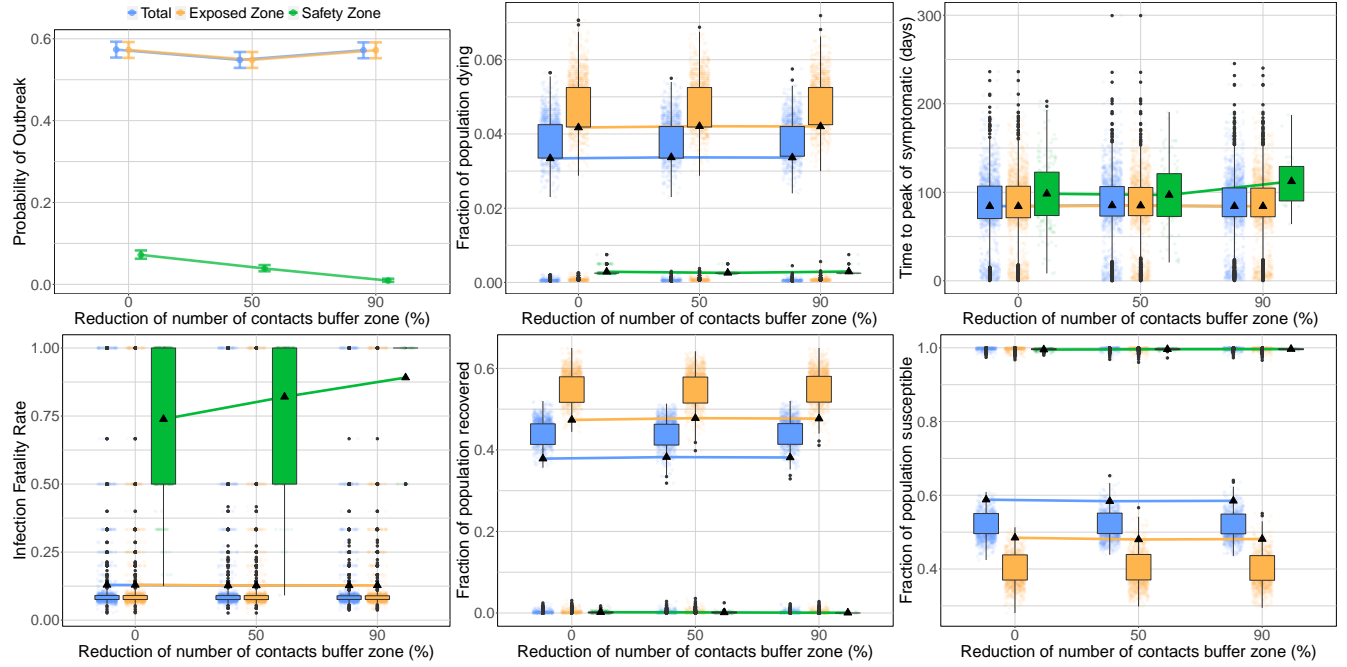


Figure 12: **Lockdown of the safety zone.** Probability of an outbreak (top left), fraction of the population dying (top middle), time until peak symptomatic cases (top right), IFR (bottom left), and fraction of the population that recovers (bottom middle) as a function of the reduction in the number of contacts permitted in the buffer zone from a baseline of 2 per person in the safety zone per week. All figures consider the scenario in which 20% of the camp's population is allocated to the safety zone.

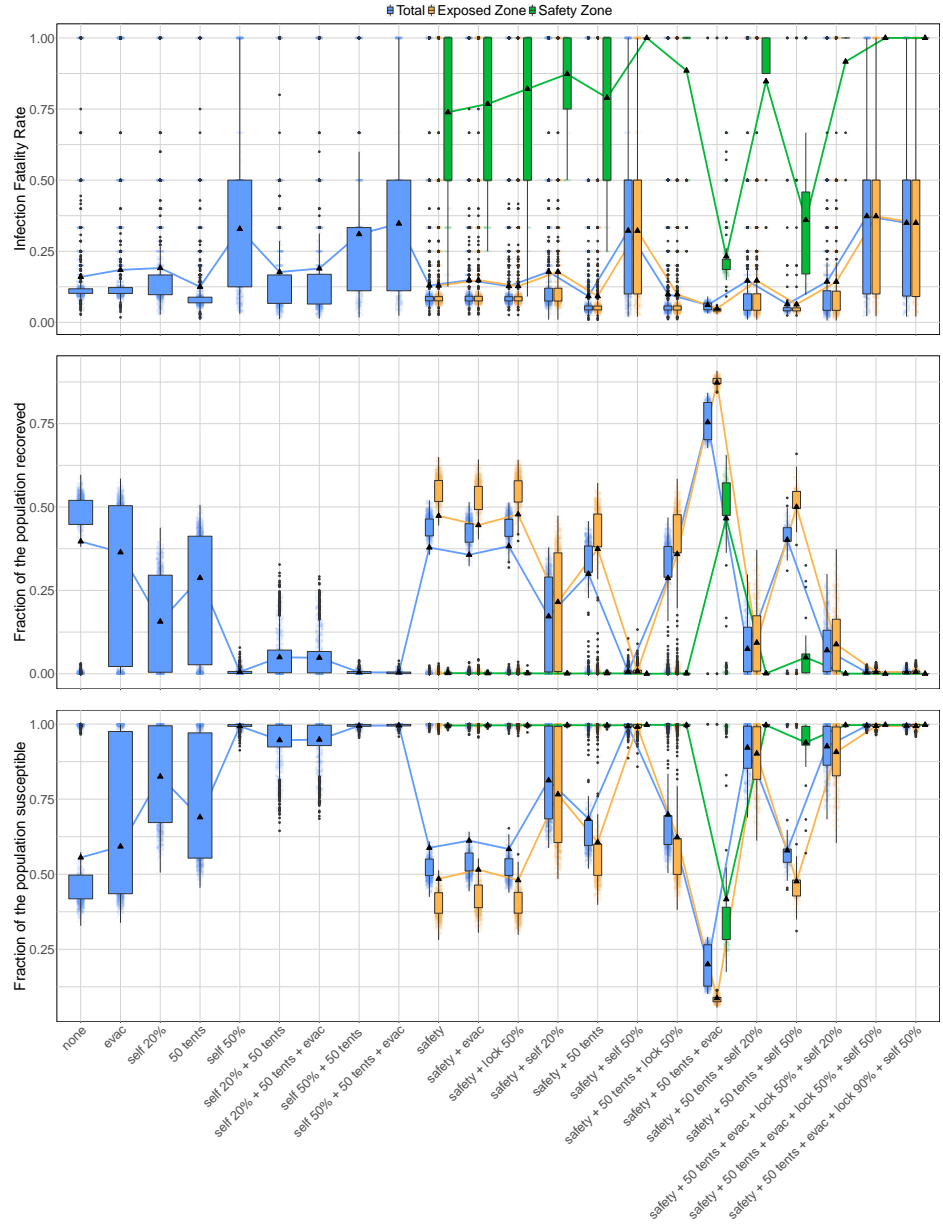


Figure 13: **Combined interventions.** IFR (top), and fraction of the population that recovers (bottom) for different combinations of interventions. Evac = evacuation of severely symptomatic, self = self-distancing, tents = number of available self-isolation tents, safety = safety zone, lock = lockdown of the buffer zone. For combinations of interventions including a safety zone, we distinguish between the population living in the green zone, in the orange zone and the whole population. The increase in the IFR for the green zone is explained by the discretization of the possible values that the IFR can take when the number of cases is very low (see Supplementary Table 3).

Intervention	<20 cases	Total	% of total
safety	16	270	5.9
safety + evac	20	249	8
safety + lock 50%	5	171	2.9
safety + self 20%	19	188	10
safety + 50 tents	11	240	4.6
safety + self 50%	14	64	22
safety + 50 tents + lock 50%	14	154	9.1
safety + 50 tents + evac	33	239	14
safety + 50 tents + self 20%	31	144	22
safety + 50 tents + self 50%	25	38	66
safety + 50 tents + evac + lock 50% + self 20%	53	110	48
safety + 50 tents + evac + lock 50% + self 50%	18	20	90
safety + 50 tents + evac + lock 90% + self 50%	6	8	75

Table 3: **Efficacy of the safety zone in combination with other interventions.** <20 cases = number of outbreaks in the green zone with fewer than 20 cases recorded. Total = total number of simulations where an outbreak in the green zone occurs (at least one death). % of total = percent of outbreaks where fewer than 20 cases are recorded. N = 500 simulations for each combination of interventions. For the most effective combinations, the majority of simulations where an outbreak occurs in the green zone see fewer than 20 cases. In these simulations, the discretization of the possible values that the IFR can take explains its apparently anomalous increase in Fig. 13.

References

- [1] Xi He, Eric HY Lau, Peng Wu, Xilong Deng, Jian Wang, Xinxin Hao, Yiu Chung Lau, Jessica Y Wong, Yujuan Guan, Xinghua Tan, et al. Temporal dynamics in viral shedding and transmissibility of COVID-19. *Nature medicine*, 26(5):672–675, 2020.
- [2] Peter Ashcroft, Jana S. Huisman, Sonja Lehtinen, Judith A. Bouman, Christian L. Althaus, Roland R. Regoes, and Sebastian Bonhoeffer. COVID-19 infectivity profile correction. *arXiv:2007.06602 [q-bio, stat]*, July 2020. arXiv: 2007.06602.
- [3] Jennifer Harcourt, Azaibi Tamin, Xiaoyan Lu, Shifaq Kamili, Senthil K Sakthivel, Janna Murray, Krista Queen, Ying Tao, Clinton R Paden, Jing Zhang, et al. Severe acute respiratory syndrome coronavirus 2 from patient with coronavirus disease, United States. *Emerging infectious diseases*, 26(6):1266, 2020.
- [4] Dawei Wang, Bo Hu, Chang Hu, Fangfang Zhu, Xing Liu, Jing Zhang, Binbin Wang, Hui Xiang, Zhenshun Cheng, Yong Xiong, et al. Clinical characteristics of 138 hospitalized patients with 2019 novel coronavirus-infected pneumonia in wuhan, china. *Jama*, 323(11):1061–1069, 2020.
- [5] Assistance Coordinator Unit. The Syrian IDP camps monitoring study - Northern Syria camps - Humanitarian Data Exchange. url: <https://data.humdata.org/dataset/idp-camps-monitoring-november-of-2018>.
- [6] Shannon Doocy, Emily Lyles, Timothy Roberton, Laila Akhu-Zaheya, Arwa Oweis, and Gilbert Burnham. Prevalence and care-seeking for chronic diseases among Syrian refugees in Jordan. *BMC Public Health*, 15(1):1097, October 2015.
- [7] Shannon Doocy, Emily Lyles, Baptiste Hanquart, Michael Woodman, and The LHAS Study Team. Prevalence, care-seeking, and health service utilization for non-communicable diseases among Syrian refugees and host communities in Lebanon. *Conflict and Health*, 10(1):21, October 2016.
- [8] Xi He, Eric H. Y. Lau, Peng Wu, Xilong Deng, Jian Wang, Xinxin Hao, Yiu Chung Lau, Jessica Y. Wong, Yujuan Guan, Xinghua Tan, Xiaoneng Mo, Yanqing Chen, Baolin Liao, Weilie Chen, Fengyu Hu, Qing Zhang, Mingqiu Zhong, Yanrong Wu, Lingzhai Zhao, Fuchun Zhang, Benjamin J. Cowling, Fang Li, and Gabriel M. Leung. Temporal dynamics in viral shedding and transmissibility of COVID-19. *Nature Medicine*, 26(5):672–675, May 2020.
- [9] Jeroen J.A. van Kampen, David A.M.C. van de Vijver, Pieter L.A. Fraaij, Bart L. Haagmans, Mart M. Lamers, Nisreen Okba, Johannes P.C. van den Akker, Henrik Endeman, Diederik A.M.P.J. Gommers, Jan J. Cornelissen, Rogier A.S. Hoek, Menno M. van der Eerden, Dennis A. Hesselink, Herold J. Metselaar, Annelies Verbon, Jurriaan E.M. de Steenwinkel, Georgina I. Aron, Eric C.M. van Gorp, Sander van Boheemen, Jolanda C. Voermans, Charles A.B. Boucher, Richard Molenkamp, Marion P.G. Koopmans, Corine Geurtsvankessel, and Annemiek A. van der Eijk. Shedding of infectious virus in hospitalized patients with coronavirus disease-2019 (COVID-19): duration and key determinants. *medRxiv*, page 2020.06.08.20125310, January 2020.
- [10] Oyungerel Byambasuren, Magnolia Cardona, Katy Bell, Justin Clark, Mary-Louise McLaws, and Paul Glasziou. Estimating the extent of asymptomatic COVID-19 and its potential for community transmission: Systematic review and meta-analysis. *Official Journal of the Association of Medical Microbiology and Infectious Disease Canada*, 5(4):223–234, December 2020.
- [11] O. Diekmann, Hans Heesterbeek, and Tom Britton. *Mathematical tools for understanding infectious diseases dynamics*. Princeton series in theoretical and computational biology. Princeton University Press, Princeton, 2013.
- [12] Sydney Philipps, Dan Rossi, Rachel Von Arb, and Alex Capaldi. Mathematical models of infectious diseases: Two-strain infections in metapopulations, July 2011.
- [13] Marino Gatto, Enrico Bertuzzo, Lorenzo Mari, Stefano Miccoli, Luca Carraro, Renato Casagrandi, and Andrea Rinaldo. Spread and dynamics of the COVID-19 epidemic in Italy: Effects of emergency containment measures. *Proceedings of the National Academy of Sciences*, 117(19):10484–10491, May 2020.
- [14] J.M Heffernan, R.J Smith, and L.M Wahl. Perspectives on the basic reproductive ratio. *Journal of the Royal Society Interface*, 2(4):281–293, sep 2005.

- [15] Yuanyuan Dong, Xi Mo, Yabin Hu, Xin Qi, Fang Jiang, Zhongyi Jiang, and Shilu Tong. Epidemiological characteristics of 2143 pediatric patients with 2019 coronavirus disease in china. *Pediatrics*, 2020.
- [16] Nancy Chow, Katherine Fleming-Dutra, Ryan Gierke, Aron Hall, Michelle Hughes, Tamara Pilishvili, Matthew Ritchey, et al. Preliminary estimates of the prevalence of selected underlying health conditions among patients with coronavirus disease 2019 in USA, february 12–march 28, 2020. *Morbidity and Mortality Weekly Report*, 69(13):382, 2020.